Performance Improvements to Wavelength Stabilized High Power 885nm Diode Laser Modules

M. Hemenway, L. Bao, M. Kanskar, M. DeVito, W. Urbanek, M. Grimshaw, K. Bruce, David. Dawson, R. Martinsen, P. Leisher

ABSTRACT

There is an increasing demand for high power diode laser packages with stabilized wavelength in the range of 878 nm to 888 nm for DPSS laser pumping applications. In this paper we present nLIGHT's most recent development of wavelength-stabilized high power, single emitter laser diode packages, *element^{TM}*, for DPSS laser pumps. We will report on how we have scaled single emitter power from 10 W per emitter with our prior generation of 200 µm wide and 3.8 mm long devices to 15 W per emitter for next generation of 5 mm cavity length device for 200 µm - 0.22 NA fiber products. The improvement in power at the chip-on-submount level results in approximately 40% increase in wavelength-stabilized power out of 200 µm fiber excited with a 0.19 NA beam, compared to the current generation *element^{TM}* products. Additionally, we will report on the improvements to wavelength-stabilization utilizing volume Bragg gratings, and chip-on-submount reliability for these new 885 nm devices, which drives the overall package reliability.

Key words: Diode reliability, fiber-coupled diode laser, wavelength stabilized, pump diodes, diode lifetime, life-test, volume Bragg grating, VBG.

1. INTRODUCTION

There has been a steady migration in the DPSS industry towards smaller diameter delivery fiber, with higher power diodes that have been wavelength stabilized to operate between 878 and 888 nm, compared to the historical pump line at 808 nm. The most recent adoption has been the use of 200 µm fiber to drive down the packaging footprint due to the smaller bend radius of the 200 µm fiber, while simultaneously driving the pump module power levels up to 150 W, or more, at the 885 nm wavelength, along with longer higher reliability. This drive has led nLIGHT to develop the largest emitting laser diode that reliably couples into 200 µm fiber with an excitation NA of 0.19. This new, wider, 885 nm laser diode, which is also available from 875 to 888 nm, is based on the 5 mm cavity length architecture we have previously reported for our 915 nm and 976 nm devices. The new 5 mm cavity length emitters is capable of 15 W output at 13.5 A, while having an estimated 23% improvement in device reliability when operated at 13 A, when compared to our current generation 3.8 mm long, 200 µm wide device operating at 10 A. This new emitter, optimized specifically for 200 µm fiber, has been demonstrated to deliver 180 W, when wavelength-stabilized with a volume Bragg grating, in nLIGHT's e18 *element^{TM}* package.

2. EMITTER OPTIMIZATION FOR 200 µm FIBER

The nLIGHT engineering team designed the widest 885 nm broad area laser, based upon our 5 mm cavity length architecture, which would reliably launch into 200 µm – 0.22 NA. This new 885 nm laser diode utilizes an improved epitaxial structure leading to low internal loss, demonstrating a 63% operational efficiency at 15W. The new design has better temperature-stability ensuing from higher efficiency and low thermal resistance, which are both critical for VBG-locked pump modules.
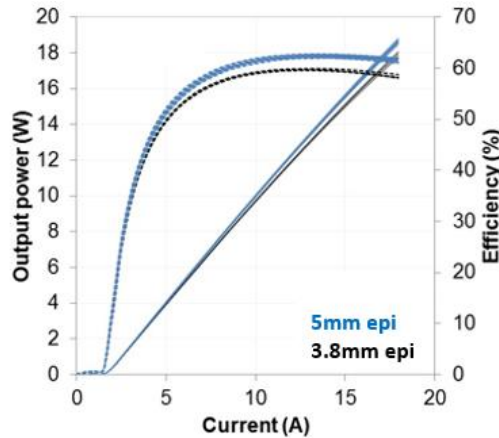
Figure 1: Power/efficiency of new 15W rated 885 nm chip with 5.0 mm laser cavity length & previous generation chip

Extensive analysis was performed comparing the power and BPP versus device reliability for several different emitter architectures. The final 5 mm design was selected to maximize reliability, power, electro-optical efficiency and wavelength stability. Generally speaking, the trend is the larger the active area of the broad area laser, the lower the current density through the junction, and therefore the "cooler running" the device is, resulting in less change in wavelength with current and reduced compliance voltage for improved electro-optical efficiency.

Initial evaluation of the 5 mm cavity length device was performed in *element*^{TM} e06 (6-emitter package) with 200 µm – 0.22 NA fiber, with results indicating the next generation 5 mm devices were performing exactly as expected, with less than 2% difference between the modeled and measured results. When packaged, we measuring 70 W output at 13A with a 51% electro-optical conversation efficiency from 7 A to 15A, prior to wavelength stabilization.
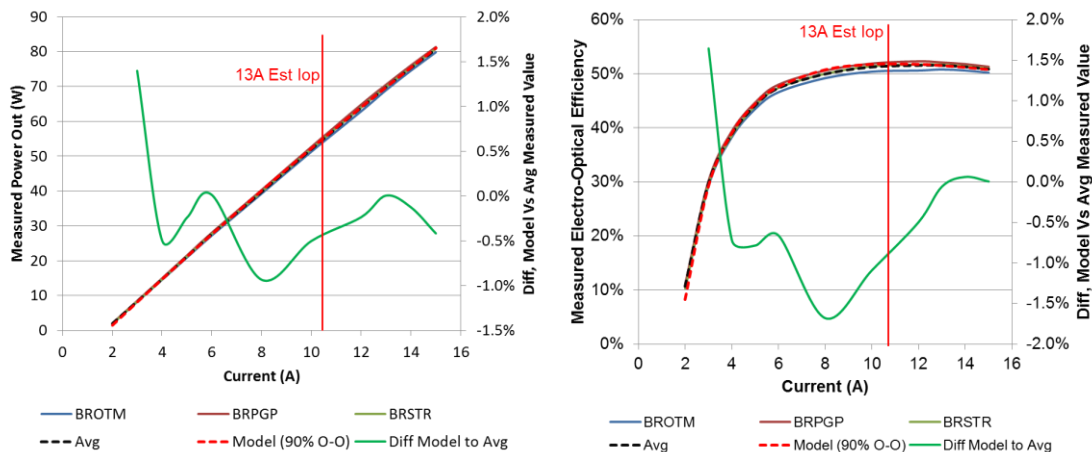
Figure 2: Measured power and electro-optical efficiency for three pre-production units, compared to modeled expectations, for the new 885 nm 5 mm cavity length emitter in a 6 emitter package with 200 µm fiber.

Additionally, for DPSS pumping it is ideal to provide the end user with a flat (super-Gaussian) far-field mode profile, so that the absorption within their gain medium is more uniform. Usually, maximizing the launch NA into the fiber provides the most uniform far-field pattern emitted from the fiber. Since the industry typically uses 0.22 NA fiber, we designed the optics and emitter architecture to result in a final packaged NA value of 0.19 when measured to the 95% power enclosure point, and 0.2 when measured to the 98% power enclosure point, with a measured value for the fiber coupling efficiency of 98%. As shown in Figure 3, not only is the NA consistent with expectations, but the emitted far-field pattern is very uniform and fits extremely well with a 6th order super-Gaussian coefficient
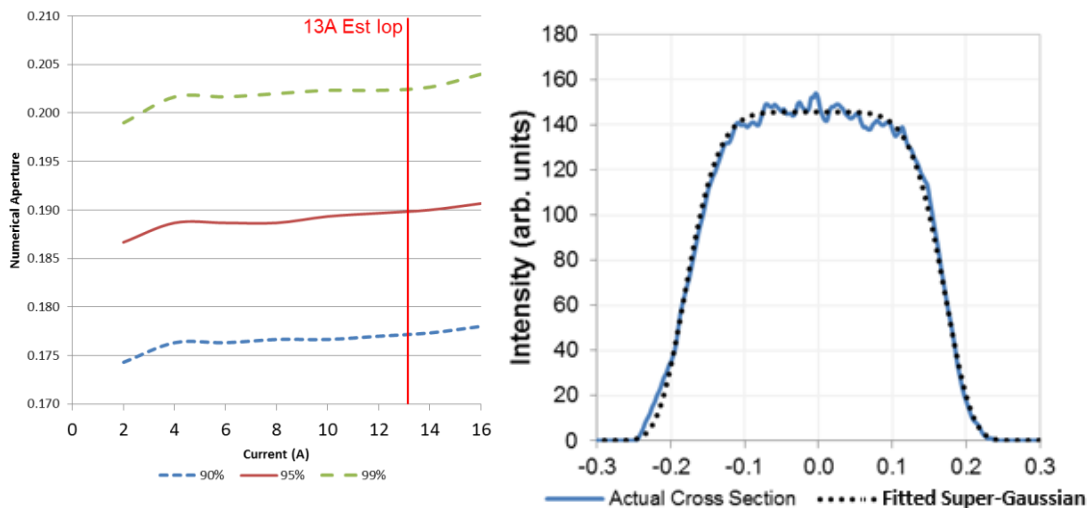
Figure 3: Measured average numerical aperture for three pre-production units, and the far-field cross section, as measured with an Ophir goniometric radiometer, for the new 885 nm 5 mm cavity length device in a 6 emitter package with 200 µm fiber.

The DPSS market also prefers wavelength-stabilized packages when utilizing devices at 878, 885 or 888 nm, so the pump spectrum remains well centered within the absorption curve of the solid state gain medium, thus improving efficiency and reducing the amount of waste heat that must be addressed. The metric commonly employed to define how well the wavelength is stabilized is Power in Band (PiB). This metric accounts for the amount of optical power contained with a certain spectral range (Spectral Radiance). A common example for this application, would be to have more than 90% of the power emitted by the pump module falling within a 2 nm (FWHM) window, and the range of currents over which the package operates under these conditions defined as the "wavelength locked" range.

After packaging the new 5 mm devices, the change in wavelength with current was measured prior to insertion of the volume Bragg grating. Generally, speaking, the lower the nm/A coefficient for a particular device, the broader the current range over which the device will remain wavelength-stabilized from the VBG.

Table 1: wavelength vs temperature coefficient for prior generation 200 µm wide, 3.8mm cavity length device compared to next generation 5mm cavity length device, when operated in *an element*^{TM} e18 package at 25 C.

Device	nm/A Coefficient
200 µm-3.8mm	1.18
Next Gen 5mm	0.59

From these measured values, it becomes obvious that for all other variables remaining equal, the next generation 5 mm cavity length laser diodes will wavelength stabilized over twice the current range of the 3.8 mm cavity length device. To validate this theory, the two devices were measured in *element*^{TM} e06 packages with 200 µm fiber, under the exact same conditions, with and without volume Bragg gratings and their performance was analyzed. It should be noted the exact same volume Bragg grating was used for each device, to eliminate grating variability from the results. In Figure 4 below, we demonstrate how the wavelength-stabilized range remains constant, in laboratory conditions, over twice the current range for the new 5 mm device compared to the 3.8mm device. It should be noted that the relative current range is not

the actual operating current of the device, but is a value that is calculated from the free-running wavelength of the device when the device temperature is increased or decreased at a given current, to shift the wavelength of the device such that it mimics the relative listed current. The lowest value was then set to 0, and the highest value is the largest relative current to the 0 value. This allows us to evaluate the theoretical range over which a device will remain wavelength stabilized when that range is much larger than the actual operating current range at 25 C. Most importantly, the new device remains wavelength stabilized over nearly 22 A of relative current range (compared to 11 A for the 3.8 mm device); for the 5 mm device which will operate between 2 A and 15 A, this means it should remain wavelength stabilized over the entire operating range when held at a constant temperature. Alternatively, this excessive range introduces additional manufacturing margin into the assembly and alignment process.
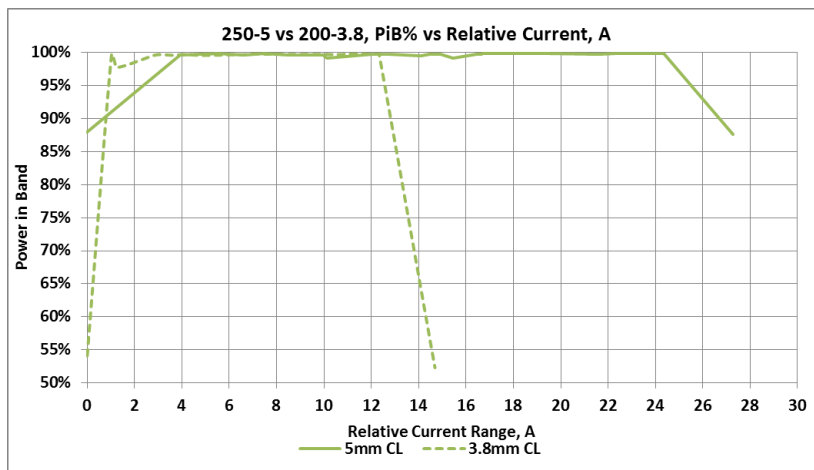
Figure 4: Relative current range over which an *element*[TM] e06 package remained wavelength stabilized with current generation 3.8mm cavity length devices vs next generation 5mm devices, using nLIGHT's standard grating reflectivity.

It should also be mentioned that device performance is strongly affected by the reflectivity of the volume Bragg grating used to wavelength stabilize the device. Lower reflectivity gratings results in less change in slope efficiency (reduced loss for higher power), but at the cost of a reduced range over which the device remains wavelength-stabilized. Tabulated below is the measured slope efficiency of the 6-emitter *element*[TM] packages, both without wavelength stabilization and with different reflectivity gratings. Each subsequent grating used in the experiment had a 4% higher reflectivity than the one preceding it. Due to the intellectual property sensitivity around this subject, the actual values have been withheld.

Table 2: 5mm and 3.8mm device slope efficiency as a function of the grating reflectivity used to wavelength stabilize the device.

	No VBG	*Lowest %R*	*Low+4%*	*Low+8%*	*Low+12%*	*Low+16%*
5mm W/A	1.05	1.03	0.98	0.94	0.91	0.85
3.8mm W/A	0.99	0.97	0.90	0.85	0.80	0.76

Since the wavelength-stabilized current range is inversely proportional to the grating reflectivity, we can now plot in Figure 5, the slope efficiency against the total relative stabilized wavelength range in Amps. From this data one can observe the new 5 mm cavity length device is clearly superior to the current generation 3.8 mm device, having improved slope efficiency and most importantly suffering less impact to slope efficiency with increasing VBG reflectivity, resulting in both significantly increased power and increased wavelength-stabilized current range. Additionally, it is observed that increasing the VBG reflectivity results in reduced device reliability due to the higher levels of feedback into the device. Thus, it is desirable from a reliability standpoint to implement the lowest reflectivity VBG which results in the desired wavelength-stabilized current range.
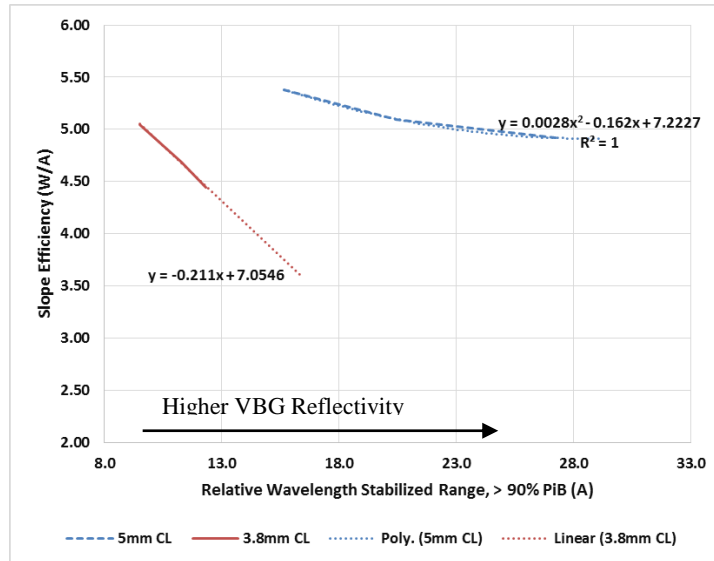
Figure 5: Slope efficiency vs locking range for 3.8mm and 5mm cavity length devices, when packaged in an *element*[TM] e06 package with 200 μm fiber.

With the new 5 mm cavity length device performance proven in the 6-emitter package, we then scaled overall package power by assembling the new 5 mm cavity length devices into an *element*[TM] e18 package. The e18 package, as reported in prior publications by nLIGHT, polarization multiplexes two banks of nine emitters into a single objective lens and delivery fiber. When operated at the estimated nominal operating current of 13 A, the measured power out for the wavelength stabilized module was an industry leading 180 W into 200 μm – 0.22 NA fiber. Additionally, the devices remained locked with greater than 97% PiB from 2A to 17 A. To the best of our knowledge, this is the highest power, wavelength stabilized pump module operating at 885 nm available.
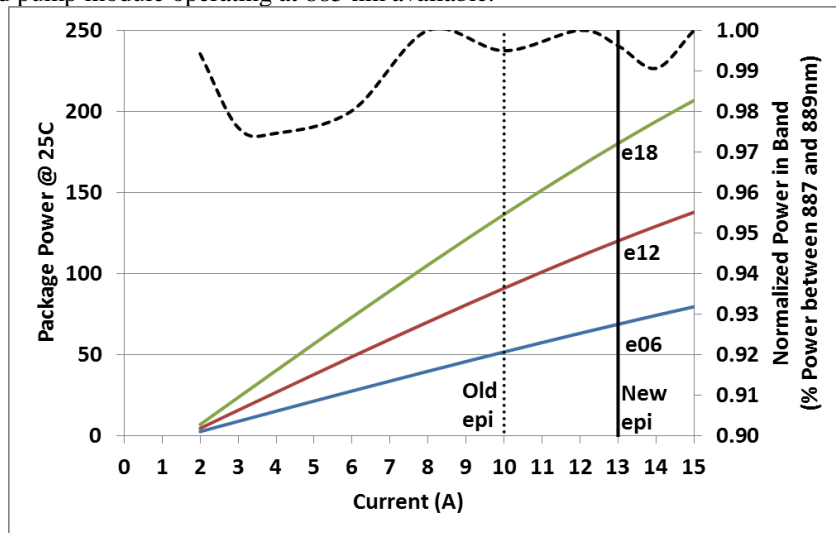
Figure 6: Measured *element*[TM] e06 and e18 package power (with extrapolated e12 power) for the new 885 nm 5 mm cavity length emitter designed for 200 μm fiber.

3. 885 nm DEVICE RELIABILITY

3.1 Multi-cell study on 6W rated 885nm diodes

One of the main advantage to perform a multi-cell lifetest with multiple accelerated stress levels is to verify the device failure statistics while simultaneously extracting the acceleration parameters. Equation (1) shows the commonly used acceleration model, which is a power law for power/current acceleration and the Arrhenius law for temperature acceleration (here P is power, I is current, T_j is junction temperature, m/n is the acceleration parameter of current/power, Ea is the activation energy and k_B is Boltzmann's constant). These acceleration parameters can then be used to predict device reliability under various operating conditions. There are limited data on the acceleration parameters and activation energy from literature, especially for state-of-the-art high power diode lasers that are produced with different material system and emitting at different wavelength.

$$\text{Acceleration Factor} \propto I^m P^n \exp\left(\frac{-E_a}{k_B \cdot T_j}\right)$$

(1)

A multi-cell life-test was started on 6W rated 885 nm single emitter laser diodes about one year ago. This multi-cell was originally designed specifically to test the wear-out mode with a highly accelerated six-cell power/temperature matrix, for the optical power in the range of 9W to 14W and junction temperatures in the range of 60°C to 90°C. The whole multi-cell was unloaded at ~9469 hours (time is slightly different for each cells) and a retest was then performed to verify failures up to this point. Failure determination is based on life-test power monitoring, retest and failure analysis. Out of 240 devices in this multi-cell, 31 devices have failed (see Table x below for failure summary). The life-test failure is verified by >=20% power degradation at retest, with failure time determined based on life-test power monitoring, retest and failure analysis. The failures were categorized into three groups based on when failure happened: life-test sudden failure, life-test degradation failure and retest failure. The life-test sudden failure is determined by a sudden power drop observed in life-test curve (power-monitoring) and confirmed by >=20% power loss by retest. The failure time of a life-test sudden failure is assigned to the instant time when power drop occurred in life-test curve. The life-test sudden failure is a very common failure mode for high power multi-mode diode lasers, which has also been observed and was the main type of failure in previously reported 910 nm to 990 nm multi-cell [4]. The life-test degradation failure is determined by a gradual power drop observed in life-test curve (power-monitoring) and confirmed by >20% power loss by retest. The failure time of a life-test degradation failure is determined as the 20% power drop time which is estimated based on a linear fit between original and retest results. The retest failure is the totally un-expected failure, as no power change was found from life-test curve while >20% power degradation was found at retest. So the failure time of retest failure is assumed to be the time at life-test unloading.

Table 3: 6W 885 nm diode multi-cell design and status

Cell #	T_j (°C)	Power (W)	Current (A)	# of failures	# of alives	Failure %	Sudden Failures	Degradation Failures	Retest Failures
1	90	14	13.8	7	33	18%	4	2	1
2	90	9	8.7	2	38	5%	1	0	1
3	60	14	13.2	8	32	20%	6	1	1
4	90	11.5	11.2	4	36	10%	3	1	0
5	70	13	12.4	3	37	8%	3	0	0
6	80	13	12.6	7	33	18%	5	2	0

A variety of failure analysis techniques were used to determine the failure mode of these 88x nm multi-cell failures and the results are summarized in Table xx. Similar to 910-990 nm and 790 nm devices, Catastrophic Optical Mirror Damage (COMD) on either PR or HR facet is still the prevalent failure mode (representing 23 failures out of 31 failures) for 885 nm diodes this multi-cell. Bulk Catastrophic Optical Damage (BCOD) is also observed, on only two failures though. It is interesting to note that three of the six degradation failures found with HR-side COMD, while the other three degradation failures do not have any obvious COD lines observed in failure analysis. The 3 failures without COD lines are actually

more typical degradation failures, which are not related to COD ran-away process, but rather related to the a nonradioactive recombination current increase due to the growth of dark spot and dark line defects [5]. Lastly, we found the three retest failures are with severe mechanical handling damage on the HR facet side, plus HR side COMD, Which is likely caused during retest after HR facet damage was introduced (at unloading operation). To be conservative, these were still included in data set as failures.

Table 4: Failure mode summary of the 6W 885 nm diode multi-cell

Cell #	PR COMD	HR COMD	BCOD	Unknown	Handling	Total	%
Lifetest Sudden Failure	18	2	2	-	-	22	71%
Lifetest Degradation Failure	-	3	-	3	-	6	19%
Retest Failure	-	-	-	-	3	3	10%
Total	18	5	2	3	3		
%	58%	16%	6%	10%	10%		

We also compared degradation in this multi-cell and found degradation is mainly observed in all cells with junction temperature at 90°C. This could indicate that the dominating failure mode might have started migrating from COMD to degradation, for diodes running at ~90°C junction temperature, as a result of less power density on the facet (for COMD failure mode) at high junction temperature, while the recombination enhanced defect generation process (for typical degradation) is believed to more current and temperature driven [5].
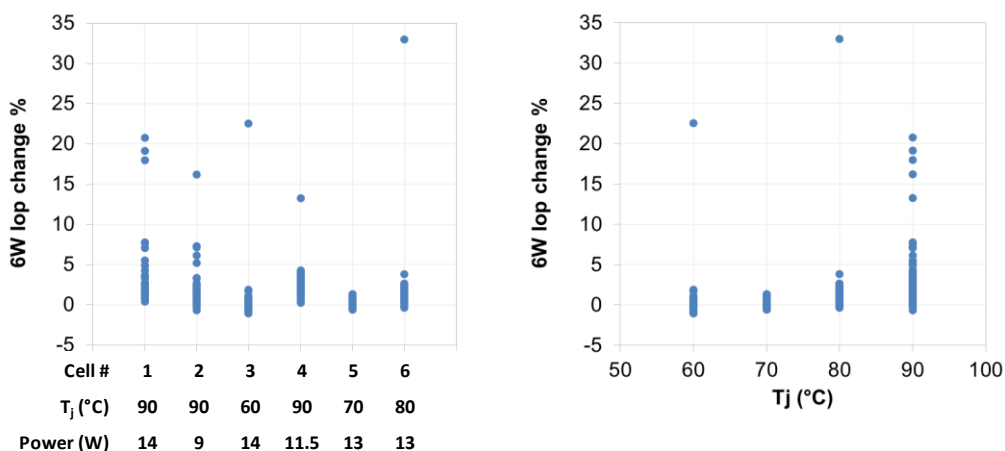
Figure 7: Retest degradation correlation (Left) with cells, (Right) with junction temperature in multi-cell

With failures and failure time determined, each multi-cell lifetest group is then separately analyzed with a 2-parameter cumulative Weibull distribution fitting, to obtain the shape factor β with 90% statistical confidence ranges (Figure 8). The shape parameter β in a 2-parameter Weibull distribution represents the failure rate change with time. $\beta = 1$ means failure rate is constant with time (random failure). $\beta < 1$ means failure rate is decreasing with time (infant mortality) and $\beta > 1$ means failure rate is increasing with time (wear-out). Based on the results summarized in Figure xx, cell 2 and cell 5 are still show $\beta \sim 1$, meaning failure rate is still about constant with time, while cell 1/3/4/6 are seeing $\beta > 1$ with 90% confidence. This suggesting these cells have some indication of increate failure rate ($\beta > 1$ with 90% confidence), though the shape parameter does not conclusively show a typical wear-out yet (typically $>= 4$).
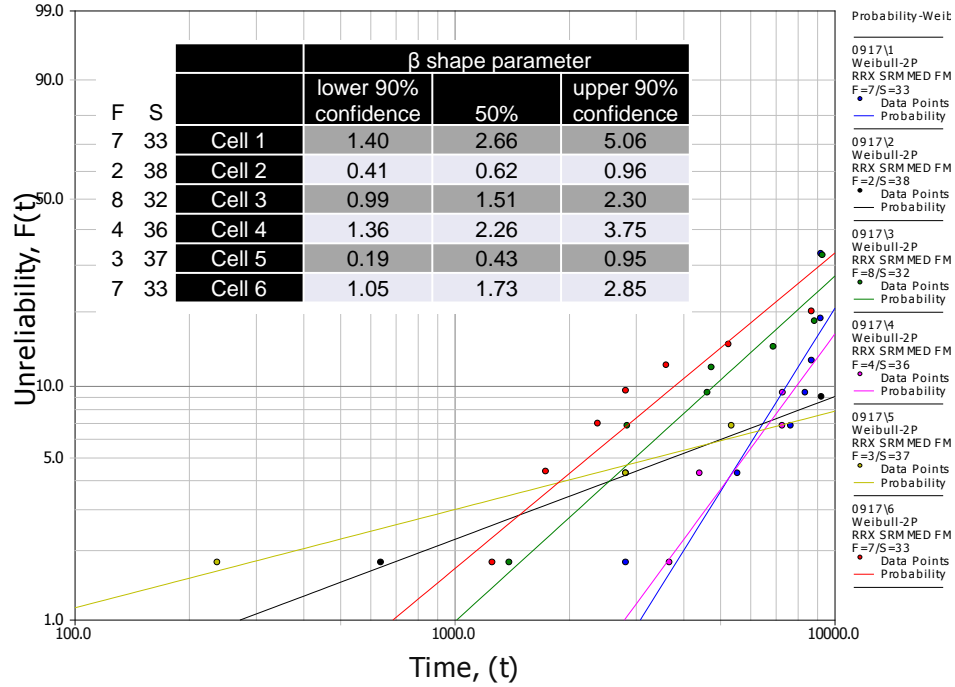
Figure 8: Weibull-2P shape parameter analysis of multi-cell results of 6W rated 885 nm laser diodes (summarized in Table 3)

Some cells with β~1(not in wear-out yet) and some cells with β just above 1(transitioning from constant failure to wear-out failure) indicate that we need more time to analyze this multi-cell for power/temperature acceleration, especially for wear-out failure. An attempt was made to analyze the power/temperature acceleration of the constant failure mode, as shown in Table 5, but the results suggest no temperature acceleration, mainly due to the conflicting results of cell 1 and cell 3. Cell 1 and cell 4 happen to be the two highest power cells (14W) in this multi-cell study. Diodes at this high power may be suggested to a new failure behavior or prune to any life-test rack power un-stability (both are just speculations though, with no proving evidence). So we decided to wait for more failures/time in each cell to separate failures from constant failures and wear-out failure mode, to conduct more meaning acceleration analysis for each case. If ignoring cell 1 and cell 3 and assuming all the failures are still constant failures, the extrapolated n (for power acceleration) and Ea (for current acceleration) is actually more close to literature published results.

Table 5: acceleration factors (Left) with all 6 cells (Right) removing 14W cell 1 and 3

All 6 cells				Only cells 2, 4, 5, 6			
Parameter	Lower 90% CL	50%	Upper 90% CL	Parameter	Lower 90% CL	50%	Upper 90% CL
Ea	-0.21	0.00	0.22	Ea	-0.36	0.36	1.07
n	0.12	2.55	4.99	n	-0.73	4.34	9.41

Finally we did the reliability analysis of this multi-cell using nominal parameters from literature, *m*=2 for current, *n*=2 for power, and E_a=0.45 eV for activation energy in equation (1). The diode reliability in this multi-cell is then plotted for 6W T$_j$ ~45C (25°C test station) operation, as in Figure 9. This multi-cell life-test data supports ~60 FIT, with 90% confidence, for 6W, 45°C junction temperature operation.

$\lambda = 5.1357E{-}8, \rho = {-}0.9077$
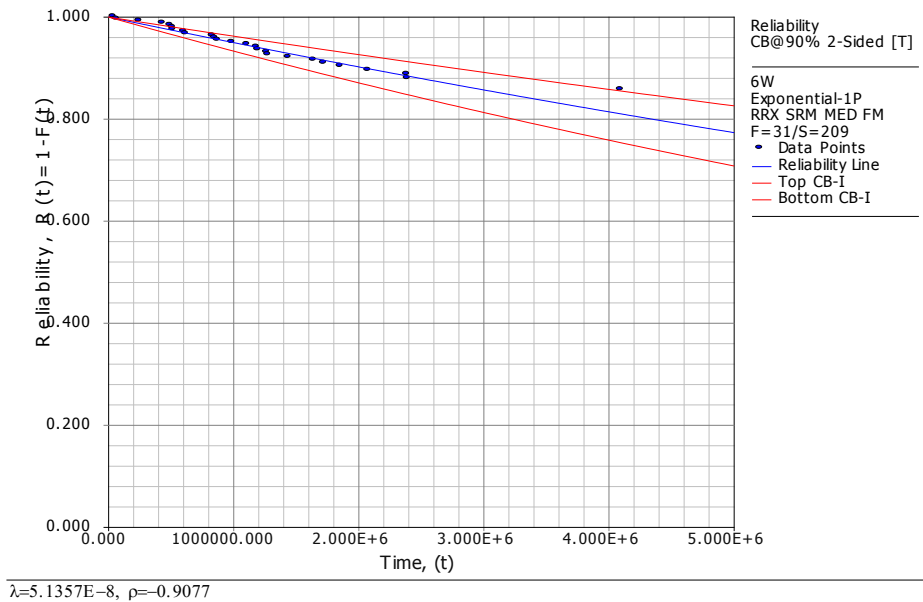
Figure 9: Reliablity of the 6W 885nm 6-cell multi-cell based on nominal acceleration factors (m=n=2 for power/current, Ea=0.45eV for temperature)

3.2 Initial reliability assessment on new 5mm long laser cavity 885 nm diodes

The new 5mm long laser cavity 885 nm design has demonstrated a better temperature-stability ensuing from higher efficiency and low thermal resistance, which are both critical for VBG-locked pump modules. For the new 5 mm cavity length devices discussed in Figure 2, we have started two rounds of accelerated reliability assessment at 20A and 70C junction temperature. So far they have accumulated about 2160h and 500 hours separately, with no failures observed (shown in Figure 10). The initial reliability assessment of these new diodes look promising. Other designated life-tests are scheduled for later this year.
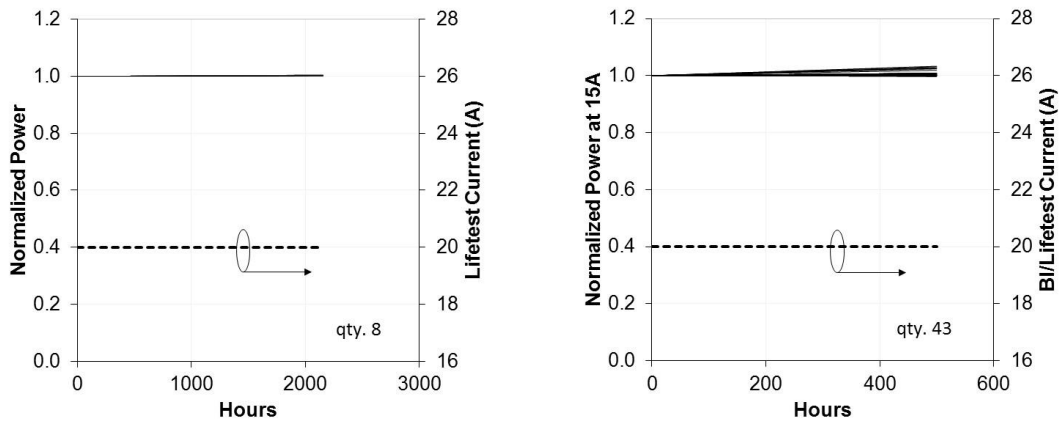
Figure 10: Two initial life-tests on new 5mm long laser cavity 885 nm diodes.

References:
[1]   K. Price, S. Karlsen, P. Leisher, R. Martinsen, "High Brightness Fiber Coupled Pump Laser Development," Proc. of SPIE 7583, 758308 (2010).

[2]   P. Leisher, K. Price, S. Karlsen, D. Balsley, D. Newman, R. Martinsen, S. Patterson, "High-Performance Wavelength-Locked Diode Lasers," Proc. of SPIE 7198, 719812 (2009).

[3]   L. Bao, J. Bai, K. Price, M. Devito, M. Grimshaw, W. Dong, X. Guan, S. Zhang, H. Zhou, K. Bruce, D. Dawson, M. Kanskar, R. Martinsen, J. Haden, "Reliability of High Power/Brightness Diode Lasers Emitting from 790 nm to 980 nm," Proc. of SPIE 8605, 860523 (2013).

[4] L. Bao, P. Leisher, J. Wang, M. DeVito, D. Xu, M. Grimshaw, W. Dong, H. Huang, S. Zhang, D. Wise, R. Martinsen, and J. Haden "High Reliability and High Performance of 9xx-nm Single Emitter Laser Diodes," Proc. of SPIE 7918, 7918-05 (2011).

[5] K. Hausler, U. Zeimer, B. Sumpf, G. Erbert and G. Trinkle, "Degradation model analysis of laser diodes," J. Mater Sci: Mater Electron 19, 160 (2008)